Design and Validation of a Lightweight Hip Exoskeleton Driven by Series Elastic Actuator With Two-Motor Variable Speed Transmission

Ting Zhang, *Member, IEEE*, Chuanxin Ning, Yang Li, and Meng Wang

***Abstract*— To overcome the different requirements of torque-velocity characteristics for walking, running, stand-to-sit, sit-to-stand, and climbing stairs, we propose a novel concept for actuator design, namely, a series elastic actuator with two-motor variable speed transmission. The two-motor variable speed transmission can be adjusted in real-time to realize variable torque-velocity characteristics. A novel lightweight wearable hip exoskeleton driven by a series elastic actuator with two-motor variable speed transmission, named SoochowExo, has been developed in this paper for use in the elderly population. The weight of the whole hip exoskeleton is 2.85 kg (excluding batteries), including two actuators and the frame. The proposed hip exoskeleton can match the weight of the state-of-the-art hip exoskeleton while offering suitable torque and velocity for sitting-to-standing, walking, running on level ground, and climbing stairs. The benchtop tests and the preliminary human subject tests further confirm the design.**

***Index Terms*— Hip exoskeleton, variable speed transmission, series elastic actuator, locomotion modes, multiple tasks.**

I. Introduction

AGING is accompanied by physical performance and sense reduction due to muscle weakness and motor unit loss [1]. The major concerns for senior citizens are handicaps related to sitting-to-standing, climbing stairs, and walking. The hip exoskeleton [2], [3], [4], [5], [6], [7], [8], [9] has become a rising research topic in recent years due to the small inertia added to the leg and the device's ability to assist elderly people in walking, sitting-to-standing, and climbing stairs. However, the current hip exoskeletons still have limitations, such as wearability, weight, and assistive performance.

Human hip joints are very important for many activities that are classified as activities of daily living (ADL), including walking, running, sitting-to-standing, climbing stairs, and the real-time adjustment of the step width to avoid falling [10], [11]. Furthermore, the hip joint has different characteristics for the different types of motion. In particular, the velocity and torque requirements for walking and sitting-to-standing are opposite. The joint needs the high torque and slow velocity of the hip flexion/extension (HFE) joints during sitting-to-standing, whereas it needs a high velocity with small torque for walking and running [12], [13]. To satisfy the requirement of high torque assistance for sitting-to-standing, most exoskeletons have been designed using high-reduce radio transmission or high-power motors [14], [15], [16]. This design will inevitably increase the inertia and weight. To improve the wearability, in addition to improving the actuator's ability, the hip exoskeleton should be as light as possible, and the structure should be slimly designed. To reduce weight, most hip exoskeletons adopt low-power motors or low reduce radio gear to meet the high-velocity requirement for walking and running. However, this will compromise the loss of the ability of high-torque assistance. Su proposed a quasi-direct drive actuation using a custom high torque density motor and low ratio gear transmission for a hip exoskeleton that demonstrates mechanical versatility for being lightweight (3.4kg overall mass), highly-backdrivable (0.4 Nm back drive torque) with high nominal torque (17.5 Nm) and high control bandwidth (62.4 Hz) [17]. However, the nominal torque of 17.5Nm is far away from the human biological hip moment requirement of the sitting-to-standing.

An exciting concept, namely, a dual reduction actuator for the knee joint of the flexible exoskeleton GEMS L-Type, has been recently introduced [18]. The two reduction radios were fixed and switched through a clutch. And the exoskeleton has to stop when the reduction radios switch. Yang, *et al.* [19] and Rouse, *et al.* [20] designed hip and knee exoskeletons so that the gear ratio can be changed during movement. Vanderborght, *et al.* [21] designed a variable stiffness actuator that used another motor to change the actuator stiffness. Horst, *et al.* [22] designed a lead screw and belt-based gear variable actuator for Orthotics. Jang designed an active-type

Manuscript received 9 May 2022; revised 15 July 2022, 12 August 2022, and 16 August 2022; accepted 21 August 2022. Date of publication 24 August 2022; date of current version 1 September 2022. This work was supported in part by the National Key Research and Development Program of China under Grant 2020YFC2007804, in part by the Natural Science Foundation of the Jiangsu Higher Education Institutions of China under Grant 19KJA180009, in part by the Natural Science Foundation of Jiangsu Province under Grant BK20191424, in part by the Jiangsu Frontier Leading Technology Fundamental Research Project under Grant BK20192004D, and in part by the Distinguished Professor of Jiangsu Province. *(Corresponding author: Ting Zhang.)*

The authors are with the Robotics and Microsystems Center, College of Mechanical and Electrical Engineering, Soochow University, Suzhou 215000, China (e-mail: zhangt.hit@gmail.com).

This article has supplementary downloadable material available at https://doi.org/10.1109/TNSRE.2022.3201383, provided by the authors.

Digital Object Identifier 10.1109/TNSRE.2022.3201383

twisted string actuator (TSA)-based on continuously variable transmission (CVT) for the robot application [23]. Lee designed a new actuator with continuously variable transmission using parallel dual-motors and a planetary gear for mobile robots [24]. Tran developed a powered knee prosthesis with actively variable transmission for multiple tasks [25], [26]. However, there has been comparatively little work on developing a hip exoskeleton with variable speed transmission to meet the different torque-velocity for the different gait tasks.

In this paper, a lightweight, compact, compliant robotic hip exoskeleton is developed for the elderly population and the population with lower-limb impairments. To overcome the different requirements of torque-velocity characteristics for walking, running, stand-to-sit, sit-to-stand, and climbing stairs, we propose a novel concept for actuator design, namely, a series elastic actuator with two-motor variable speed transmission. The speed transmission ratio can be adjusted in real-time to realize variable torque-velocity characteristics. Furthermore, two-motor variable speed transmission can adapt to elderly people's personalized motion characteristics due to age and physical condition.

The main contributions of this paper are as follows:

1) introduce the concept of the series elastic actuator with two-motor variable speed transmission to the hip exoskeleton design to meet the different requirements of torque-velocity characteristics for walking, running, stand-to-sit, sit-to-stand, and climbing stairs;

2) develop a novel lightweight, wearable hip exoskeleton driven by series elastic actuator with two-motor variable speed transmission, named SoochowExo, to promote the independent living of the elderly and the population with lower-limb impairments.

The paper is structured as follows. The hardware and controller design are described in Sections II and III. Section III and V present the bench-top testing and the preliminary human subject tests, which show the performance of the SoochowExo. The discussion and conclusion are described in Sections VI and VII, respectively.

II. Hardware Design

A. Design Objectives

The main objective of the hip exoskeleton is to assist the elderly and the population with lower-limb impairments in sitting-to-standing, walking, running, and climbing stairs. The actuator requirements of torque and speed are different for different locomotion modes, such as walking, running, stand-to-sit, sit-to-stand, and climbing stairs [13], [27], [28]. The actuators of hip exoskeleton are required to working in distinctively different torque-speed load conditions. To achieve this, a series elastic actuator with two-motor variable speed transmission is designed to meet the different requirements for the assistive torque and velocity. The peak torque and velocity are designed to meet the velocity requirement, gain higher torque output, and reduce the weight. To ensure a wide range of speeds, the actuator's requirement of the hip exoskeleton firstly is to have high velocity, and then can offer large assistive torque for the sitting-to-standing and slow walking. The design requirements of the hip exoskeleton are summarized in Table I. The hip exoskeleton was designed to offer assistive torque of 60 Nm with the velocity of 2.3rad/s at the highest transmission ratio, while output torque of 12Nm with the velocity of 5.6rad/s at the lowest transmission ratio.

TABLE I
SUMMARIZES THE HIP EXOSKELETON DESIGN GOALS

	target	actual
Total active DOFs	Hip flex. /ext.	Hip flex. /ext.
Speed transmission ratio range	6:1 ~ 32:1	6:1 ~ 32:1
Peak torque range (Nm)	12 ~ 60	12 ~ 62
Peak velocity range (rad/s)	5.6 ~ 2.3	5.9 ~ 2.8
Actuator	SEA	SEA
Weight (excluding the power supply system)	As light as possible	2.85 kg

(a) Frame of the hip exoskeleton

(b) System overview of the hip exoskeleton

Fig. 1. System overview of the proposed hip exoskeleton: SoochowExo.

B. Design Overview

Fig. 1 shows the overall system of the hip exoskeleton. This hip exoskeleton is designed to deliver assistive torque to both HFE joints. The hip exoskeleton includes the flexible suit and two module actuators that can connect to the flexible suit. The hip exoskeleton consists of a pair of series elastic actuators with two-motor variable speed transmission for the HFE joints, and a pair of 3D-print customized frames. The layout of the hip exoskeleton is designed to minimize the extra inertia on the wearer's limb and maximize wearing comfort. The interface between the hip exoskeleton and the wearer consists of four parts: a belt to conform to the wearer's waist shape, two braces for both thighs, and a suspender. The two actuators, the embedded control system, and the battery are located close to the back, which is in the proximity of the center of mass of the

TABLE II
THE MATERIAL AND WEIGHT FOR DIFFERENT PARTS OF THE HIP EXOSKELETON

Item	Quantity	Material	weight
Actuator with link	2	aluminum alloy	0.875
Brace	2	Plastic, textile	0.15
Suspender	1	textile	0.1
Frame	2	plastic	0.2
Belt	1	fabric	0.2
Circuit	1	-	0.1
Total		2.85kg	

wearer. The overall hip exoskeleton system weight without a battery is 2.85 kg. The material and weight for different parts of the hip exoskeleton are shown in Table II.

The hip exoskeleton includes the following core elements:

1) Two-motor variable speed transmission: To meet the assistance of various tasks, such as level-walking and sitting-to-standing, the transmission ratio of the HFE actuators of the hip exoskeleton could continue to change adaptively. The series elastic actuator with two-motor variable speed transmission uses a novel transmission system that adapts the actuator torque and speed to the demand of different ambulation tasks. For example, the speed transmission ratio adjusts to high for tasks that require high torque and low speed, such as sitting-to-standing tasks, and adjusts to low for tasks that require high speed with low output torque, such as walking and running.

2) Series elastic actuator (SEA): The actuator is designed based on the SEA concept presented in our previous works [7]. The SEA configuration can realize accurate interaction force control and complaint interaction with the wearer, as well as the torque sensor, which measures the displacement under the load.

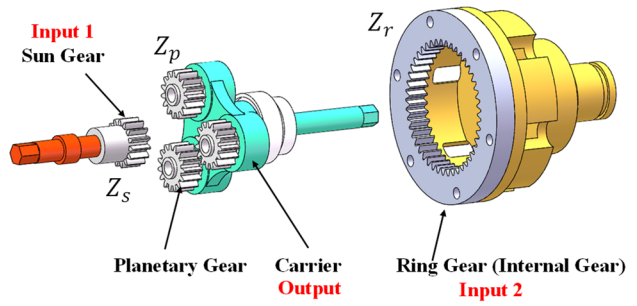

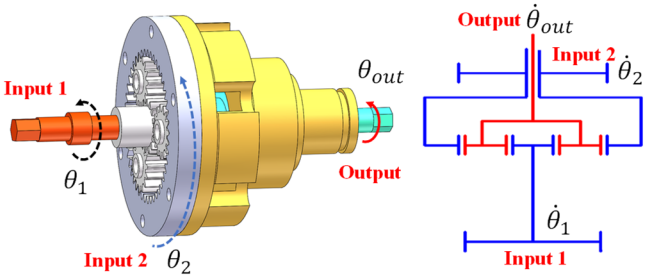

Fig. 2. Basic concept of two-motor variable speed transmission.

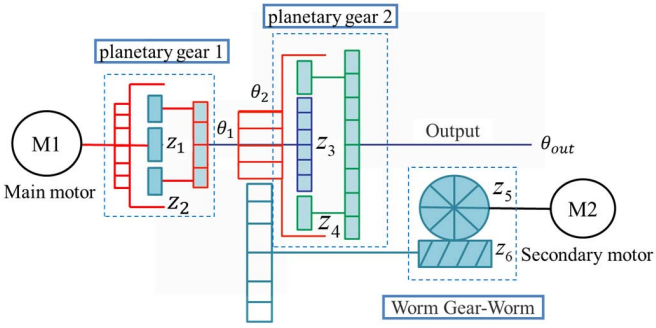

Fig. 3. Schematic diagram of the transmission system.

C. The Principle of the Two-Motor Variable Speed Transmission

The principle of the two-motor variable speed transmission for the hip exoskeleton is based on the planetary gear mechanism. A planetary gear includes four parts: sun gear, ring gear, planet gears, and carrier. There have two motion control inputs, one is the sun gear and the other is the ring gear rotation, to adjust the rotation speed of the carrier and the planet gears, as shown in Fig. 2.

When the ring gear is fixed ($\dot{\theta}_2 = 0$), the velocity relation between the input 1 and output is:

$$\dot{\theta}_{out} = \left(\frac{Z_s}{Z_s + Z_r}\right)\dot{\theta}_1 \tag{1}$$

When the sun gear is connected with input 1 and the ring gear is connected with input 2, the output velocity $\dot{\theta}_{out}$ can be expressed as

$$\dot{\theta}_{out} = \left(\frac{Z_s}{Z_s + Z_r}\right)\dot{\theta}_1 + \left(\frac{Z_r}{Z_s + Z_r}\right)\dot{\theta}_2 \tag{2}$$

where Z_s, Z_p, and Z_r is the number of sun gear teeth, the planetaries teeth, and the ring gear teeth, respectively.

Fig. 3 shows the concept of the planetary gear-based two-motor variable speed transmission in our design. Two planetary gear subsystems are series-connected together in the two-motor variable speed transmission. The basic principle is that two inputs contribute to one output. The first planetary gear's reduction ratio is constant, while the second planetary gear's reduction ratio is determined by two inputs θ_1 and θ_2. The main input θ_1 comes from the output of the first planetary gear and is connected to the sun gear of the second planetary stage. The second input θ_2 is connected to the ring gear. A worm and gear driven by the small-power motor were applied at the input θ_2 to change the reduction ratio of actuators and can also provide a self-locking function.

When the small-power motor is powered off ($\dot{\theta}_{m2} = 0$), the two-motor variable speed transmission worked in the highest-transmission ratio mode. The speed transmission ratio R_H is:

$$\dot{\theta}_{out} = \frac{z_3}{z_3 + z_4}\dot{\theta}_1 \tag{3}$$

$$\dot{\theta}_1 = \frac{z_1}{z_1 + z_2}\dot{\theta}_{m1} \tag{4}$$

$$R_H = \frac{z_1 \cdot z_3}{(z_1 + z_2)(z_3 + z_4)} \tag{5}$$

When the $\dot{\theta}_2$ rotated in the opposite direction to the main drive motor, then Two motor variable speed transmission worked in the low-transmission ratio mode. The speed

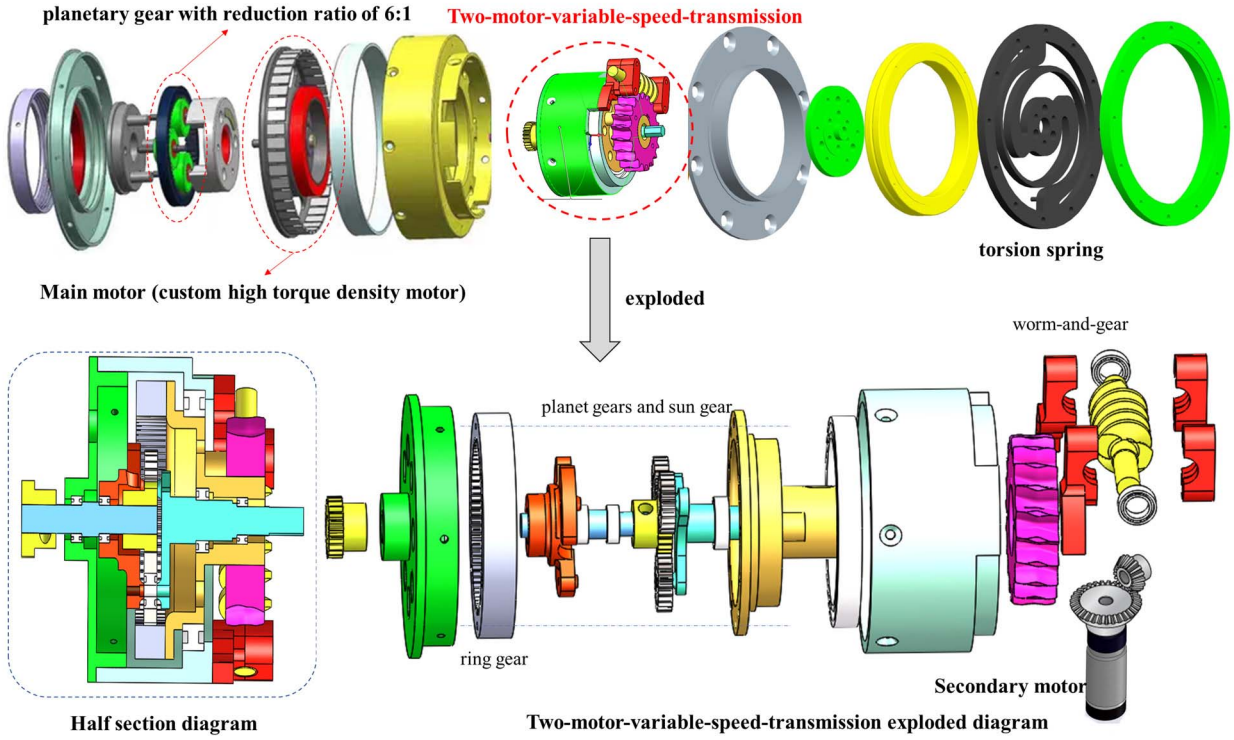

Fig. 4. CAD of the SEA-with-two-motor-variable-speed-transmission.

transmission ratio R_L is computed as follows:

$$\dot{\theta}_{out} = \frac{z_3}{z_3 + z_4}\dot{\theta}_1 - \frac{z_4}{z_3 + z_4}\dot{\theta}_2 \tag{6}$$

$$\dot{\theta}_1 = \frac{z_1}{z_1 + z_2}\dot{\theta}_{m1} \tag{7}$$

$$\dot{\theta}_2 = \frac{z_5}{z_6}\dot{\theta}_{m2} \tag{8}$$

$$\dot{\theta}_{m2} = k\dot{\theta}_{m1} \tag{9}$$

$$R_L = \frac{z_1 \cdot z_3 \cdot z_6 - z_4 \cdot z_5 \cdot k \cdot (z_1 + z_2)}{(z_1 + z_2)(z_3 + z_4)z_6} \tag{10}$$

where z_1, z_2 are the number of sun gear teeth and ring gear teeth of the planetary gear 1, respectively, z_3, z_4 are the number of sun gear teeth and ring gear teeth of the planetary gear 2, respectively, z_5, z_6 is the number of worms and worm gear teeth, respectively, k is proportion factor of the velocity between the main motor and secondary motor.

D. Fully-Integrated SEA-With-Two-Motor-Variable-Speed-Transmission

Fig. 4 shows the CAD of the SEA-with-two-motor-variable-speed-transmission. The system consists of the main motor, secondary motor, two planetary gear modules, two motor variable speed transmission, and strings. The main motor is directed connected with the sun gear of the first planetary gear module using a coupler. The carrier of the first planetary gear module was mounted next to the two-motor variable speed transmission. The two-motor variable speed transmission includes a sun gear, ring gear, three planet gears, a carrier, a worm-and-gear, and a secondary motor. The output of the first planetary gear module is connected with the sun gear of the two-motor variable speed transmission. The ring gear of the two-motor variable speed transmission connected with the second motor through a worm-and-gear.

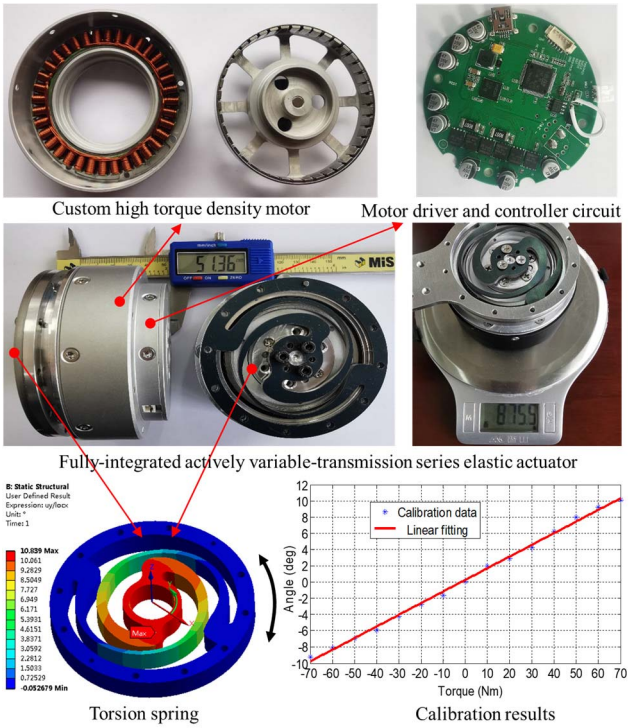

Fig. 5. Fully-integrated SEA-with-two-motor-variable-speed-transmission.

Fig. 5 shows the fabricated fully-integrated SEA-with-two-motor-variable-speed-transmission with dimensions of

Ø90 mm × 51mm. The overall actuator weight is 680 g (actuator with link weight is 875 g), including the main motor and second motor, two planetary gear-based two-motor variable speed transmission systems, and two high-resolution encoders. Furthermore, the motor driver and STM32 microcontroller-based embedded control system are integrated into the actuator as a module.

To meet the small dimension, lightweight, high power density ratio requirements of hip exoskeleton design, a custom high torque density motor (Our motor was manufactured by Unitree Robotics) was adopted into our design to work as the main motor of the SEA-with-two-motor-variable-speed-transmission. The customized high torque density motor (280 g), which can output nominal torque of 2 Nm with a normal speed of 2100 RPM works as the main input q_{m1} of the two-motor variable speed transmission.

The second input q_2 of the two-motor variable speed transmission is driven through a small power DC motor (EC10, Maxon, Sachseln, Switzerland), a harmonic gear drive (HDUC-5-80-1U-CC, Harmonic Drive, Limburg, Germany), and a worm-and-gear with a reduction ratio of 75:1 (MÄDLER, modulus of 0.5 mm). This motor and transmission ratio configure can ensure the maximum velocity of the second input q_2 make the output $\dot{\theta}_{out}$ in the (5) equal to zero, then the SEA-with-two-motor-variable-speed-transmission work at the lowest-transmission mode.

Considering assistive torque and velocity requirements during level running and sitting-to-standing, we chose the gear parameters z_1, z_2, z_3, z_4, z_5, and z_6. The relative ratio between the maximum low- transmission and high- transmission modes for the hip exoskeleton was set to 4. The transmission ratio reached 32:1 in the highest-transmission mode, and the resulting output torque reached 64 Nm with a nominal velocity of 5.6 rad/s. In the low-transmission mode, we set the small-power motor motion at maximum speed, resulting in the minimum reduction ratio for the HEF joint being 6:1. The resulting nominal velocity was up to 25 rad/s with an output torque of 16 Nm. The lowest-transmission mode allows the wearer to run up to 2.5 m/s with 20% biological torque assistance.

Furthermore, the series elastic actuator concept was also used in the design. There is a customized torsion spring serving as an elastic element sandwich between the output of the transmission and the torque output. This SEA configuration can realize accurate torque control and complaint interaction, as well as the torque sensor [8], [29]. The designed stiffness of the monolithic disc-shaped torsion spring is 400 Nm/rad. The maximum of the deformation and torque is ±10° and ±60Nm, respectively. The torsion spring, with a high-resolution quadrature kit encoder (Avago AEDA-3300 Series, Broadcom Limited, South Carolina) is needed to measure the deflection; it also operates as a torque sensor with a resolution of 0.03 Nm.

III. Controller Design

A. Embedded System

The hip exoskeleton includes the onboard and off-board custom electronic boards. The onboard custom electronic circuit is devoted to controlling and driving the motors (two motors for the HFE joint, and one motor for the step-width adjustment joint), collecting data on the encoders, and CAN bus communication. The chip of the onboard embedded system is STM32 32-bit Arm Cortex MCUs. The onboard embedded system is integrated into the modular joint, as shown in Fig. 5.

The off-board and battery are placed at the back of the exoskeleton. One DSP chip (TMS320F2812)-based embedded system operates controllers that read all sensor data to compute high-level control algorithms. The high-level controller communicates with a motor controller that is integrated into the actuators through a CAN bus. There are two IMUs on both thighs to estimate the acceleration of hip flexion/extension and adduction/abduction. There is one more IMU placed at the back to measure the angles, velocity, and acceleration of the upper body.

B. Low-Level Torque Control of the SEA-With-Two-Motor-Variable-Speed-Transmission

For the low-level controller, the controller performs closed-looped torque tracking control of the SEA-with-two-motor-variable-speed-transmission. The torque sensor data measured by the deformation of the torsion spring are fed back to the low-level controller. The torque control is transformed into the torsion spring's deflection control:

$$\tau_d(\theta) = k\theta_s \tag{11}$$

where θ_s is the torsion spring's deflection, and k is the stiffness of the torsion spring.

The torsion spring's deflection control is based on the proportional-integral differential (PID) controller. Reference torque signal is the input and is converted into a command spring deflection angle for the feedback term. The output of the PID torque controller is the desired velocity $\dot{\theta}_{out}$. Then we can get the control command of the main motor and secondary motor through:

$$\dot{\theta}_{out} = \frac{z_4}{z_3 + z_4} \cdot \frac{z_1}{z_1 + z_2}\dot{\theta}_{m1} - \frac{z_3}{z_3 + z_4} \cdot \frac{z_5}{z_6}\dot{\theta}_{m2} \tag{12}$$

C. High-Level Assistive Control

The hip exoskeleton works in various modes, such as level walking (LW), stair ascent (SA), stair descent (SD), sitting-to-standing, and standing-to-sitting. The relationship between the assistive timing and the gait cycle is different for the various locomotion modes inspired by the human hip joint biological torque [30], [31]. The control goal is to offer effective assistive torque to adapt to the different locomotion modes. Starting from the heel strike ($\theta_{heel-strike}$), the controller generates the desired assistive torque. The assistive torque profile is a mixture of four halves of minimum jerk curves joined together at their tops, as shown in Fig. 6.

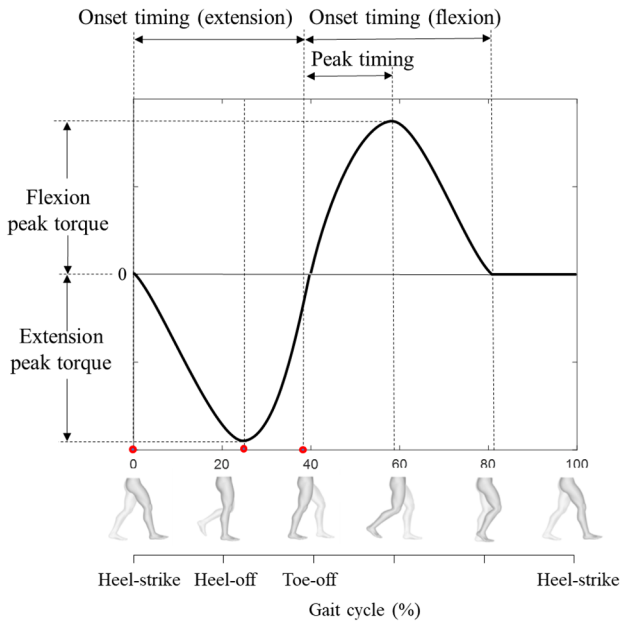

Fig. 6. Parameterization of the hip torque profile.

The assistive torque profile is:
when $\theta_{heel-strike} \leq \theta < \theta_{heel-off}$,

$$\tau_d(\theta) = \tau_{p\_e} - 2\tau_{p\_e}\left(\frac{\theta_{heel-off} - \theta}{\theta_{heel-off} - \theta_{heel-strike}}\right)^2 + \tau_{p\_e}\left(\frac{\theta_{heel-off} - \theta}{\theta_{heel-off} - \theta_{heel-strike}}\right)^3 \quad (13)$$

when $\theta_{heel-off} \leq \theta < \theta_{toe-off}$,

$$\tau_d(\theta) = 3\tau_{p\_e}\left(\frac{\theta_{toe-off} - \theta}{\theta_{toe-off} - \theta_{heel-off}}\right)^2 - 2\tau_{p\_e}\left(\frac{\theta_{toe-off} - \theta}{\theta_{toe-off} - \theta_{heel-off}}\right)^3 \quad (14)$$

when $\theta_{toe-off} \leq \theta < \theta_{p\_f}$,

$$\tau_d(\theta) = \tau_{p\_f} - 2\tau_{p\_f}\left(\frac{\theta_{p\_f} - \theta}{\theta_{p\_f} - \theta_{toe-off}}\right)^2 + \tau_{p\_f}\left(\frac{\theta_{p\_f} - \theta}{\theta_{p\_f} - \theta_{toe-off}}\right)^3 \quad (15)$$

when $\theta_{p\_f} \leq \theta < \theta_{offset\_f}$,

$$\tau_d(\theta) = 3\tau_{p\_f}\left(\frac{\theta_{offset} - \theta}{\theta_{offset} - \theta_{p\_f}}\right)^2 - 2\tau_{p\_f}\left(\frac{\theta_{offset} - \theta}{\theta_{offset} - \theta_{p\_f}}\right)^3 \quad (16)$$

otherwise

$$\tau_d(\theta) = 0 \quad (17)$$

where $\tau_d(\theta)$ is the assistive torque; $\theta_{heel-strike}$, $\theta_{heel-off}$, and $\theta_{toe-off}$ are the hip angles corresponding to gait events of the heel strike, heel off, and toe-off, respectively; τ_{p_f} and τ_{p_e} are the flexion and extension peak torques, respectively; θ_{p_f} is the hip flexion angle corresponding to the assistive torque at the peak timing; and θ is the hip joint angle. The gait cycle begins and ends at the heel-strike event. θ_{onset} is maximum flexion angle, which is an average value based on previous strides measured through IMUs [32]. The proposed assistive torque profile mimics the human biological hip moment profile. Over a gait cycle, the assistive torque profile can generate an assistive torque for both hip flexion and extension. Three parameters, θ_{p_f}, τ_{p_f} and τ_{p_e}, are adjusted in real-time to adapt to the different locomotion modes (LW, SD, SA, running) and the different speeds. θ_{p_f} is defined as follows:

$$\theta_{p\_f} = A \cdot \theta_{onset} \quad (18)$$

where A is a constant, which is to determine the hip flexion assistive torque onset timing (increasing from toe-off and end at the maximum flexion angle) in the gait cycle. And A will be set as different values for the LW, running, SD, and SA. The onset timing is determined by the gait events. τ_{p_f} and τ_{p_e} are scaled for the different locomotion modes. Additionally, τ_{p_f} and τ_{p_e} are also scaled for different walking speeds and benefits from the actuator being able to actively vary the reduction ratio. The three key parameters (A, τ_{p_f} and τ_{p_e},) can dictate the assistance profile that is offset timing, assistance duration, and assistance magnitude.

IV. Benchtop Experiments

A. Backdrivability and Zero-Torque Control Performance of the SEA-With-Two-Motor-Variable-Speed-Transmission

We conducted benchtop testing and quantified the performance in terms of the torque and velocity capabilities and backdrivability. The fully integrated SEA-with-two-motor-variable-speed-transmission was fixed during the benchtop experiments. The output shaft of the actuator was manually pushed. The torque and angle data are measured through a spring-based toque sensor and encoders.

In the first test, the actuator was working in the highest-reduction ratio mode, both motor M1 and M2 are power off. Fig. 7 (a) shows the relationship between the back-drive torque and the angle. The proposed hip exoskeleton's passive compliance is due to the elasticity introduced by the customized torsion spring. In the second test, SEA-with-two-motor-variable-speed-transmission worked at close-looped zero torque control to testing the active compliance. The back-drive torque of the fully integrated SEA-with-two-motor-variable-speed-transmission within 0.1 Nm for the different motion frequencies, as shown in Fig. 7 (b).

B. Closed-Loop Torque Control Bandwidth With Different Reduction Ratio

To test the torque and velocity characteristics of the fully integrated series elastic actuator with two-motor variable speed transmission, the actuator was velocity-controlled motion with different loadings. The peak torque can reach 12 Nm when the actuator operates in the lowest-transmission ratio mode (6:1), and the normal velocity is more than 5.9 rad/s. The actuator is operated with a peak torque of 62 Nm and a normal velocity

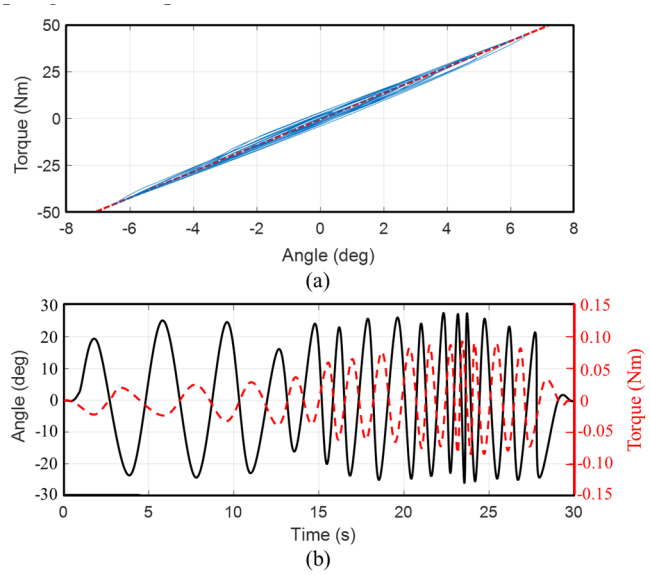

Fig. 7. Backdrivability Experiment. (a) The actuator worked at the highest-reduction ratio mode (the stiffness of the SEA), (b) closed-looped zero torque control.

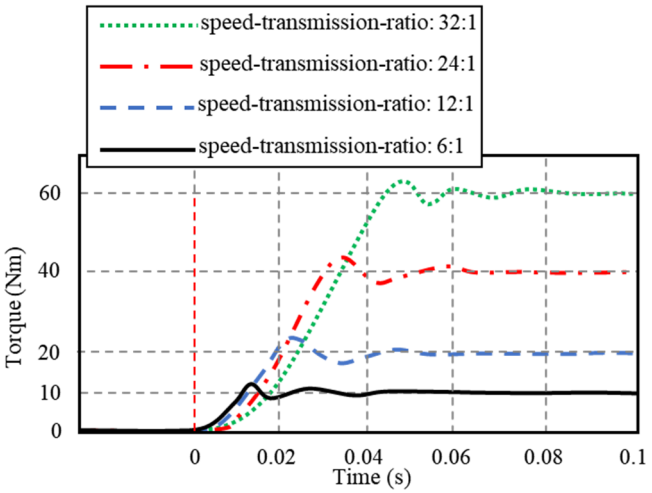

Fig. 8. Step response of the torque control.

TABLE III
THE PERFORMANCE OF THE ACTUATOR WITH DIFFERENT TRANSMISSION RATIOS

	6: 1	12: 1	24: 1	32: 1
Peak Torque (Nm)	12	23	46	62
Peak velocity (rad/s)	5.9	5.18	3.75	2.8
Cutoff frequency (Hz)	43.75	29.17	19.44	12.52
Transmission ratio adjusting time (increasing) (ms)	→	13±4	28±5	21±3
Transmission ratio adjusting time (decreasing) (ms)	11±4	24±3	17±5	←

of 2.8 rad/s when operating in the highest-transmission ratio mode (32:1).

Step response tests were performed for the SEA-with-two-motor-variable-speed-transmission with the output of the device rigidly fixed. The output of the SEA-with-two-motor-variable-speed-transmission was blocked while step responses were tested (i.e., 10 Nm, 20 Nm, 40 Nm, and 60 Nm), as shown in Fig. 8. Table III summarized the performance of the actuator with different speed transmission ratios. For the SEA-with-two-motor-variable-speed-transmission, the cut-off frequency of the closed-loop torque control is 43.75 Hz, 29.17 Hz, 19.44 Hz, and 12.52 Hz at 10 Nm, 20 Nm, 40 Nm, and 60Nm, respectively. We also test the adjustment time of the speed transmission ratio increasing from 6:1 to 12:1, 24:1, and 32:1, and then decreasing from 32:1 to 24:1, 12:1, and 6:1 five times. The adjustment time is 13±4, 28±5, and 21±3s for increasing from 6:1 to 12:1, from 12:1 to 24:1, and from 24:1 to 32:1, respectively. And the adjustment time is 17±5, 24±3, and 11±4s for decreasing from 32:1 to 24:1, from 24:1 to 12:1, and from 12:1 to 6:1, respectively.

C. Continual Torque Control of the SEA-With-Two-Motor-Variable-Speed-Transmission

In this experiment, the proposed SEA-with-two-motor-variable-speed-transmission torque and velocity characteristics are examined in the condition that the speed transmission ratio continually adjusting, while outside of SEA-with-two-motor-variable-speed-transmission is interacted with an external motion. A high-power motor (300W) with a reduction gear of 200:1 was used as external motion. A commercial torque sensor is connected between the SEA-with-two-motor-variable-speed-transmission and external motion to measure the load torque.

Test 1: The SEA-with-two-motor-variable-speed-transmission is controlled to track a torque increased from 0Nm to 60 Nm within the 60 s, while the external motor is braked.

Test 2: The SEA-with-two-motor-variable-speed-transmission is controlled to track a torque increased from 0Nm to 60 Nm within the 60 s, while the external motor with a fixed speed of 3 rad/s.

Test 3: The SEA-with-two-motor-variable-speed-transmission is controlled to track a fixed torque of 10 Nm, while the external motion is increased from 0 rad/s to 10 rad/s within the 60 s.

The SEA-with-two-motor-variable-speed-transmission output torque, the velocity and current of the main and secondary motor, and external motion velocity were recorded. Fig. 11 shows the test results, from top to the bottom (Fig. 9 (a)- Fig. 9 (c)) is the results of *Test 1*, *Test 2*, and *Test 3*. For *Test 1*, as shown in Fig. 9 (a), we can see that only the main motor M1 motion. The SEA-with-two-motor-variable-speed-transmission worked at the highest-transmission ratio mode. The motor current increased with torque increasing. For *Test 2*, as shown in Fig. 9 (b), the secondary motor M2 began motion at T1 and stopped at T2 to adjust the reduction ratio to meet both the torque and velocity requirements. For *Test 3*, as shown in Fig. 9 (c), the secondary motor M2 began motion at T1 to adjust the reduction ratio.

V. PRELIMINARY HUMAN SUBJECT TESTS

Five healthy subjects (age 28.5±6 y.o., weight 78.5±9.9 kg, height 1.76±0.26 m) participated in the preliminary human

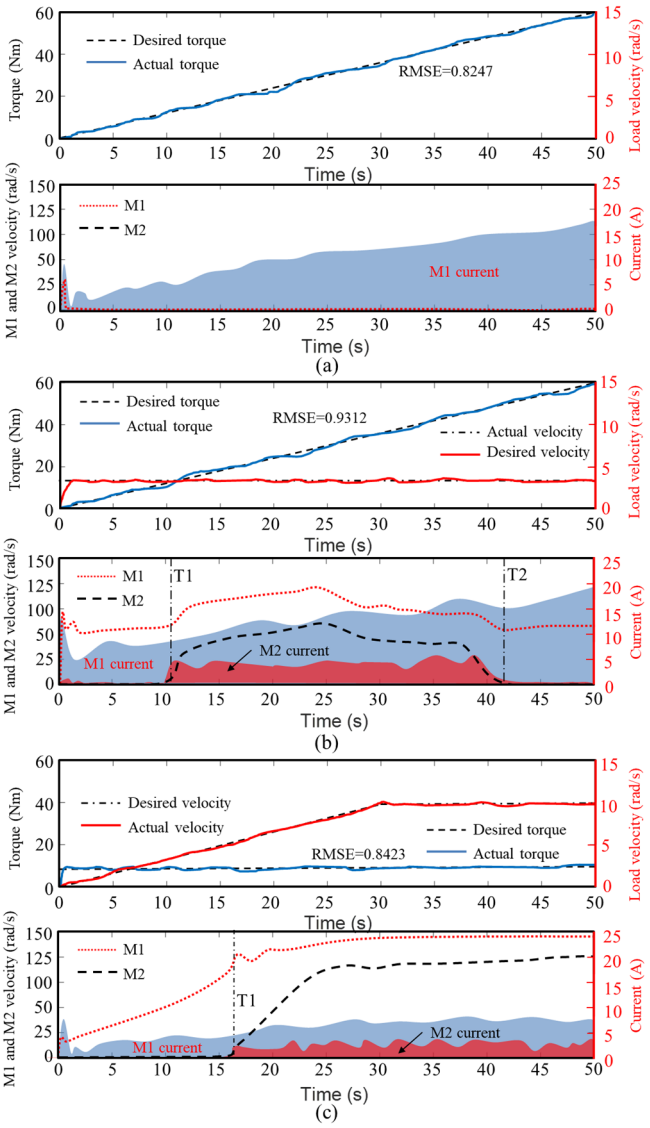

Fig. 9. Continual torque control. Note: The M2 velocity in the plots is the harmonic gear drive output side's velocity. (a) Test 1, (b) Test 2, (c) Test 3.

subject tests. All subjects signed an informed consent form. The experiments were approved by the Ethical Committee of Soochow University. The hip exoskeleton was powered by a lithium-ion battery (400 g), which can support the device in operation for 1.5 hours. The actuator, electric circuit, and battery were fixed in the bag, which was fixed at the wearer's back.

The hip joint angle and assistive torque of the hip exoskeleton were recorded to analyze the performance of the assistance. The hip joint angles and assistive torque were measured by an encoded spring-based torque sensor integrated into a fully integrated series elastic actuator with actively variable reduction ratio transmission. The hip angles during the free motion were performed without wearing the hip exoskeleton (*no exo*) and were measured through an inertial motion capture system (Perception Neuron 2.0, Noitom Technology Ltd.). The heel-strike event, which was detected through two loading cells placed at each shoe, was used to normalize the gait periods.

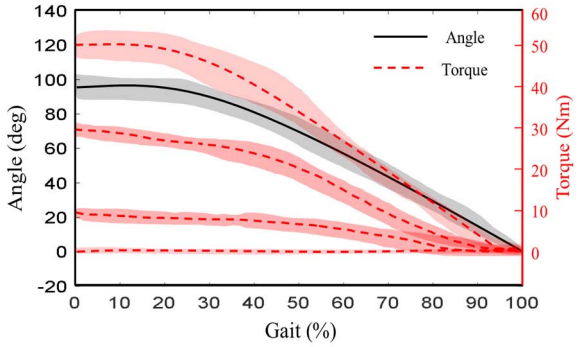

Fig. 10. Sit-to-Stand transition experiment.

A. Sit-to-Stand Test

The subjects wore the hip exoskeleton and performed sit-to-stand trials with different peak torque assistances. The subjects were asked to keep the same speed to sitting-to-standing at each trial. For the sitting-to-standing, the assistive torque profile is:

$$\tau_d(\theta) = 3\tau_{peak}\left(\frac{\theta_{stand}-\theta}{\theta_{stand}-\theta_{sit}}\right)^2 - 2\tau_{peak}\left(\frac{\theta_{stand}-\theta}{\theta_{stand}-\theta_{sit}}\right)^3 \tag{19}$$

where τ_{peak} is the peak assistive torque, θ_{stand} is the hip flexion angle when the human stands, and θ_{sit} is the hip flexion angle when the human sits. We set θ_{stand} to 5 degrees; the hip exoskeleton will work in zero torque mode when the hip flexes and is smaller than 5 degrees, which allows the subject to freely move. The peak assistive torque was set as 50 Nm, 30 Nm, 10 Nm, and 0 Nm (power off) for the four test groups.

Fig. 10 shows the HFE joint angle, assistive torque under the peak assistive torque was set as 50 Nm, 30 Nm, 10 Nm, and 0 Nm (power off). There were no significant changes in the hip HFE joint angle on the peak assistive torque was set as 50 Nm, 30 Nm, 10 Nm, and 0 Nm (power off). We can see from Fig. 8 that the assistive torques start from the beginning sitting on the chair and are gradually reduced to zero with standing. The assistive torques show that the hip exoskeleton can output assistive torque up to 50 Nm.

B. Different Locomotion Modes Assistance Tests

The subjects walked on a treadmill for 10 min at a fixed speed of 1.2 m/s, ran on a treadmill for 10 min at a fixed speed of 2.2 m/s, and ascended and descended a stair (four floors, 230 stairs) under three conditions: wearing the hip exoskeleton with assistance (*assist on*), wearing the hip exoskeleton without assistance (*assist off*), and without wearing the hip exoskeleton (*no exo*) [35]. Participants were asked to keep the selected cadences constant during the ascending stair and descending stairs. We set A as different values for LW, SA, SD, and running based on the human biological hip moment [12], [13].

Fig. 11 shows the average kinematic and assistive force delivered by the hip exoskeleton under three conditions: *assist on*, *assist off*, and *no exo*. Fig. 11 shows that the assistive torque begins at the heel-strike event, smoothly increases

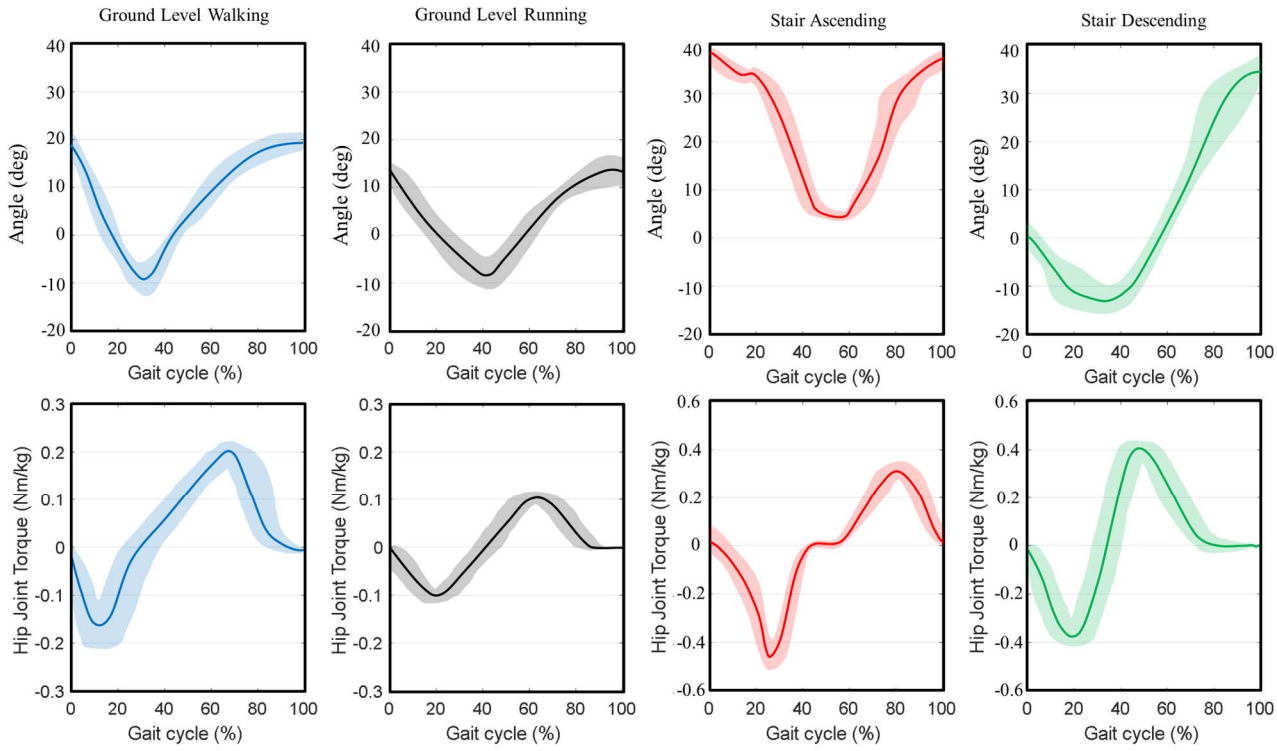

Fig. 11. The results of the different locomotion modes assistance tests.

TABLE IV
ASSISTANCE PARAMETERS FOR THE DIFFERENT LOCOMOTION MODES

	τ_{p_f}	τ_{p_e}	A	Speed
LW	0.2Nm/kg	-0.2Nm/kg	65%	1.2 m/s
SA	0.3Nm/kg	-0.5Nm/kg	20%	-
SD	0.4Nm/kg	-0.4Nm/kg	30%	-
Running	0.1Nm/kg	-0.1Nm/kg	20%	2.2m/s

τ_{p_f} and τ_{p_e} are the flexion and extension peak torque, respectively, A is a constant, which is to determine the hip flexion assistive torque onset timing (increasing from toe-off and end at the maximum flexion angle) in the gait cycle.

TABLE V
PERFORMANCE OF ASSISTANCE FOR THE DIFFERENT LOCOMOTION MODES

	LW	Running	SA	SD
Angle (deg)	(-14, 23)	(-12, 18)	(4, 39)	(-14, 37)
Peak torque (Nm/kg)	0.22	0.12	0.53	0.42
Peak velocity (rad/s)	2.43	5.48	2.98	3.21
Torque tracking error (RMSE)	0.189	0.234	0.201	0.209

to the negative peak and ends at heel-off, then increases to the positive peak and ends at maximum hip flexion for all locomotion modes. Table V summarized the performance of hip exoskeleton assistance for the different locomotion modes. The peak torque reached 0.22 Nm/kg, 0.12 Nm/kg, 0.53 Nm/kg, 0.42 Nm/kg and 0.21 Nm/kg and 0.12 Nm/kg, 0.32 Nm/kg, and 0.42 Nm/kg at extension and flexion for walking, running, SA, and SD, respectively. The assistive torque up to peak flexion torque reached 20%, 20%, 30%, and 40% for the walking, running, SA, and SD, respectively, while up to extension torque at 20%, 20%, 30%, 40%. In summary, the hip exoskeleton only introduced minimum changes to gait kinematics. The assistive force tracked the designed profiles for different locomotion modes. Furthermore, the assistive torque could also adapt to different subjects' independent walking speeds.

VI. DISCUSSION

The design of hip exoskeletons for elderly individuals is challenging in terms of the weight of the exoskeleton, the compromise between force and velocity, the comfortable wearer–exoskeleton interface, and assistance performance. The hip joints work together on many activities, such as sitting-to-standing, walking, running, and climbing stairs. There are diverse characteristics of the different activities. The torque and velocity requirements for walking/running and sitting-to-standing are opposite. The motivation of this paper is to address this opposite and to avoid using a high-power motor to reduce the weight of the hip exoskeleton.

Benefitting the planetary gear's multiport characteristics, a series elastic actuator with two-motor variable speed transmission is designed for our hip exoskeleton, which can support different speed transmissions. In the lowest- transmission ratio mode, the transmission ratio for the HFE joints is 6:1. Based on our benchtop tests, the peak velocity is more than 5.9 rad/s with an output torque of 16 Nm, which allows the wearer to run at 2.5 m/s, as shown in Fig. 11. In contrast, in the highest-transmission ratio mode, the transmission ratio for the HFE joints becomes 32:1. The resulting peak torque can reach 60 Nm, which can assist sitting-to-standing with 25% of the biological hip flexion torque, as shown in Fig. 10. Based on the two-motor variable speed transmission and custom high torque density motor, the fully integrated SEA weighing 870 g can generate assistive torque up to 60 Nm

in the highest-transmission ratio mode and can allow the hip exoskeleton to run at a high speed of 2.5 m/s in the lowest-reduction mode. These performances are achieved by adopting a high torque density motor and two-motor variable speed transmission rather than using a high transmission ratio or high-power motor due to their inherent heavy and bulky characteristics.

The proposed SEA-with-two-motor-variable-speed-transmission can continuously adjust the speed transmission ratio similar to [26], and not only discretely adjust between tasks like [25], [26], and [18]. Different from the two same motor parallel arranged input to the planetary gear in [24], there has a high-power motor work as the main input to output the drive torque, and a low-power motor with the worm-and-gear as secondary input work to adjust the speed transmission ratio. Different from [24], the reduction ratio of the proposed SEA-with-two-motor-variable-speed-transmission is reduced with the increasing velocity of the secondary motor. Furthermore, there have two planetary gears series connections as the variable speed transmission. These configure reduced the axial dimension and the weight of the actuator. Besides, our two-motor variable speed transmission connected with a torsion spring assemble as a series elastic actuator to realize accurate interaction force control and complaint interaction with the wearer, as well as the torque sensor.

The proposed wearable hip exoskeleton with the two-motor variable speed transmission series elastic actuator is to promote the independent living of the elderly and the population with lower-limb impairments. The SEA-with-two-motor-variable-speed-transmission can meet the individual needs of the elderly because different elderly people and people with lower-limb impairments have different assistance level requirements. Furthermore, our exoskeleton also has the potential to reduce joint loadings of non-disabled populations for regular activities. The motivation of this paper is to propose an actuator design concept for the hip exoskeleton. The speed transmission ratio adjusts rang can choose based on the user's requirement.

Whatever how our effort, the hip exoskeleton still introduces nonnegligible mass. Currently, the hip exoskeleton focuses on reducing the weight to assist energy-efficient walking, which hasn't a frame to support the weight. A biomechanics study [34] showed that the energy expenditure increased the smallest when additional loading was applied to the waist compared with the thigh, shank, or foot. The energy expenditure will not significantly increase when the 4 kg mass loading is at the waist. The proposed hip exoskeleton is 2.85 kg (excluding batteries). And this weight is light than the most of hip exoskeletons [4], [6], [7], [8], [9], [15], [16]. Our hip exoskeleton with the rigid frame can connect with the weight support frame, such as Kim designed bio-inspired knee joint [35] or Lenzi designed self-aligning mechanism [36], to balance the weight of the exoskeleton, it will be beneficial for the elderly to wear the hip exoskeleton long time.

Several limitations related to the device's design and controls still limit the possibility of adoption without extra work. There is a tradeoff between the actuator's backdrivability and the two-motor variable speed transmission. The backdrivability of the SEA-with-two-motor-variable-speed-transmission depends on the stiffness of the customized torsion spring when both motor M1 and M2 power off. The back-drive torque is big than [17], [37]. A simplistic control scheme was used in this paper to evaluate the performance of the hip exoskeleton during steady-state walking, running, SA, SD, RA, and RD. The peak timing and peak force were fixed. Previous studies [38] have shown that online peak force and timing optimization can improve gait performance and reduce energy expenditure. The load cells at the shoes were used in the controller to detect the gait event and introduce cables at the shoes and legs. In the future, detecting gait events based on IMUs placed on the thighs will eliminate cable issues. With the design of the hip exoskeleton now validated, additional elderly people and people with lower-limb impairments clinical validation can conduct investigate clinical outcomes in the further [39].

VII. Conclusion

In this paper, a novel concept for actuator design, namely, a series elastic actuator with two-motor variable speed transmission is introduced in the hip exoskeleton design. The reduction ratio can be adjusted in real-time to meet the different requirements of torque-velocity characteristics for walking, running, stand-to-sit, sit-to-stand, and climbing stairs. The design, control, and experimental validation of a novel lightweight hip exoskeleton for elderly individuals and people with lower-limb impairments are presented in this study. The proposed lightweight hip exoskeleton driven by SEA-with-two-motor-variable-speed-transmission can application in elderly people and people with lower-limb impairments, as well as the able-bodied populations for regular activities.

References

[1] P. T. Chinimilli, S. M. R. Sorkhabadi, and W. Zhang, "Assessment of human dynamic gait stability with a lower extremity assistive device," *IEEE Trans. Neural Syst. Rehabil. Eng.*, vol. 28, no. 3, pp. 669–678, Mar. 2020.

[2] F. Giovacchini *et al.*, "A light-weight active orthosis for hip movement assistance," *Robot. Auton. Syst.*, vol. 73, pp. 123–134, Nov. 2015.

[3] K. Yasuhara, K. Shimada, T. Koyama, T. Ido, K. Kikuchi, and Y. Endo, "Walking assist device with stride management system," *Honda R D Tech. Rev.*, vol. 21, no. 2, pp. 57–66, 2009.

[4] Q. Wu, X. Wang, F. Du, and X. Zhang, "Design and control of a powered hip exoskeleton for walking assistance," *Int. J. Adv. Robotic Syst.*, vol. 12, no. 3, pp. 1–11, 2015.

[5] A. T. Asbeck, K. Schmidt, and C. J. Walsh, "Soft exosuit for hip assistance," *Robot. Auton. Syst.*, vol. 73, pp. 102–110, Nov. 2015.

[6] T. Zhang, M. Tran, and H. Huang, "Admittance shaping-based assistive control of SEA-driven robotic hip exoskeleton," *IEEE/ASME Trans. Mechatronics*, vol. 24, no. 4, pp. 1508–1519, Aug. 2019.

[7] T. Zhang and H. Huang, "Design and control of a series elastic actuator with clutch for hip exoskeleton for precise assistive magnitude and timing control and improved mechanical safety," *IEEE/ASME Trans. Mechatronics*, vol. 24, no. 5, pp. 2215–2226, Oct. 2019.

[8] I. Kang, D. D. Molinaro, S. Duggal, Y. Chen, P. Kunapuli, and A. J. Young, "Real-time gait phase estimation for robotic hip exoskeleton control during multimodal locomotion," *IEEE Robot. Autom. Lett.*, vol. 6, no. 2, pp. 3491–3497, Apr. 2021.

[9] M. K. Ishmael, D. Archangeli, and T. Lenzi, "Powered hip exoskeleton improves walking economy in individuals with above-knee amputation," *Nature Med.*, vol. 27, no. 10, pp. 1783–1788, Oct. 2021.

[10] M. K. Ishmael, M. Tran, and T. Lenzi, "ExoProsthetics: Assisting above-knee amputees with a lightweight powered hip exoskeleton," in *Proc. IEEE 16th Int. Conf. Rehabil. Robot. (ICORR)*, Jun. 2019, pp. 925–930.

[11] Y. Lee *et al.*, "Biomechanical design of a novel flexible exoskeleton for lower extremities," *IEEE/ASME Trans. Mechatronics*, vol. 22, no. 5, pp. 2058–2069, Oct. 2017.

[12] M. Grimmer and A. Seyfarth, "Mimicking human-like leg function in prosthetic limbs," in *Neuro-Robotics*. Berlin, Germany: Springer, 2014, pp. 105–155.

[13] D. A. Winter, "The biomechanics and motor control of human gait: Normal, elderly and pathological," *J. Biomech.*, vol. 25, no. 8, p. 949, 1992.

[14] A. M. Dollar and H. Herr, "Lower extremity exoskeletons and active orthoses: Challenges and state-of-the-art," *IEEE Trans. Robot.*, vol. 24, no. 1, pp. 144–158, Feb. 2008.

[15] T. Yan, M. Cempini, C. M. Oddo, and N. Vitiello, "Review of assistive strategies in powered lower-limb orthoses and exoskeletons," *Robot. Auto. Syst.*, vol. 64, pp. 120–136, Feb. 2015.

[16] A. J. Young and D. P. Ferris, "State of the art and future directions for lower limb robotic exoskeletons," *IEEE Trans. Neural Syst. Rehabil. Eng.*, vol. 25, no. 2, pp. 171–182, Feb. 2017.

[17] S. Yu *et al.*, "Quasi-direct drive actuation for a lightweight hip exoskeleton with high backdrivability and high bandwidth," *IEEE/ASME Trans. Mechatronics*, vol. 25, no. 4, pp. 1794–1802, Aug. 2020.

[18] Y. Lee *et al.*, "Flexible gait enhancing mechatronics system for lower limb assistance (GEMS L-type)," *IEEE/ASME Trans. Mechatronics*, vol. 24, no. 4, pp. 1520–1531, Aug. 2019.

[19] I. Kang, H. Hsu, and A. Young, "The effect of hip assistance levels on human energetic cost using robotic hip exoskeletons," *IEEE Robot. Autom. Lett.*, vol. 4, no. 2, pp. 430–437, Apr. 2019.

[20] M. K. Shepherd and E. J. Rouse, "Design and validation of a torque-controllable knee exoskeleton for sit-to-stand assistance," *IEEE/ASME Trans. Mechatronics*, vol. 22, no. 4, pp. 1695–1704, Aug. 2017.

[21] T. Bacek, M. Moltedo, C. Rodriguez-Guerrero, J. Geeroms, B. Vanderborght, and D. Lefeber, "Design and evaluation of a torque-controllable knee joint actuator with adjustable series compliance and parallel elasticity," *Mechanism Mach. Theory*, vol. 130, pp. 71–85, Dec. 2018.

[22] R. W. Horst and R. R. Marcus, "FlexCVA: A continuously variable actuator for active orthotics," in *Proc. Int. Conf. IEEE Eng. Med. Biol. Soc.*, Aug. 2006, pp. 2425–2428.

[23] J. Jang, Y.-U. Song, and J.-H. Ryu, "Active-type continuously variable transmission system based on a twisted string actuator," *IEEE Robot. Autom. Lett.*, vol. 7, no. 2, pp. 2605–2612, Apr. 2022.

[24] H. Lee and Y. Choi, "A new actuator system using dual-motors and a planetary gear," *IEEE/ASME Trans. Mechatronics*, vol. 17, no. 1, pp. 192–197, Feb. 2012.

[25] M. Tran, L. Gabert, M. Cempini, and T. Lenzi, "A lightweight, efficient fully powered knee prosthesis with actively variable transmission," *IEEE Robot. Autom. Lett.*, vol. 4, no. 2, pp. 1186–1193, Apr. 2019.

[26] T. Lenzi, M. Cempini, L. Hargrove, and T. Kuiken, "Design, development, and testing of a lightweight hybrid robotic knee prosthesis," *Int. J. Robot. Res.*, vol. 37, no. 8, pp. 953–976, Jul. 2018.

[27] D. A. Winter, "Biomechanical motor patterns in normal walking," *J. Motor Behav.*, vol. 15, no. 4, pp. 302–330, Dec. 1983.

[28] S. R. Hamner and S. L. Delp, "Muscle contributions to fore-aft and vertical body mass center accelerations over a range of running speeds," *J. Biomech.*, vol. 46, pp. 780–787, Feb. 2012.

[29] T. Zhang, M. Tran, and H. Huang, "Design and experimental verification of hip exoskeleton with balance capacities for walking assistance," *IEEE/ASME Trans. Mechatronics*, vol. 23, no. 1, pp. 274–285, Feb. 2018.

[30] X. Liu and Q. Wang, "Real-time locomotion mode recognition and assistive torque control for unilateral knee exoskeleton on different terrains," *IEEE/ASME Trans. Mechatronics*, vol. 25, no. 6, pp. 2722–2732, Dec. 2020.

[31] W. Huo, S. Mohammed, Y. Amirat, and K. Kong, "Fast gait mode detection and assistive torque control of an exoskeletal robotic orthosis for walking assistance," *IEEE Trans. Robot.*, vol. 34, no. 4, pp. 1035–1052, Aug. 2018.

[32] Y. Ding, I. Galiana, C. Siviy, F. A. Panizzolo, and C. Walsh, "IMU-based iterative control for hip extension assistance with a soft exosuit," in *Proc. IEEE Int. Conf. Robot. Autom. (ICRA)*, Stockholm, Sweden, May 2016, pp. 3501–3508.

[33] J. Kim *et al.*, "Reducing the metabolic rate of walking and running with a versatile, portable exosuit," *Science*, vol. 365, no. 6454, pp. 668–672, 2019.

[34] R. C. Browning, J. R. Modica, R. Kram, and A. Goswami, "The effects of adding mass to the legs on the energetics and biomechanics of walking," *Med. Sci. Sports Exerc.*, vol. 39, no. 3, pp. 515–525, 2007.

[35] T. Kim, M. Jeong, and K. Kong, "Bioinspired knee joint of a lower-limb exoskeleton for misalignment reduction," *IEEE/ASME Trans. Mechatronics*, vol. 27, no. 3, pp. 1223–1232, Jun. 2022.

[36] S. V. Sarkisian, M. K. Ishmael, and T. Lenzi, "Self-aligning mechanism improves comfort and performance with a powered knee exoskeleton," *IEEE Trans. Neural Syst. Rehabil. Eng.*, vol. 29, pp. 629–640, 2021.

[37] H. Zhu, C. Nesler, N. Divekar, V. Peddinti, and R. D. Gregg, "Design principles for compact, backdrivable actuation in partial-assist powered knee orthoses," *IEEE/ASME Trans. Mechatronics*, vol. 26, no. 6, pp. 3104–3115, Dec. 2021.

[38] Y. Ding, M. Kim, S. Kuindersma, and C. J. Walsh, "Human-in-the-loop optimization of hip assistance with a soft exosuit during walking," *Sci. Robot.*, vol. 3, no. 15, Feb. 2018, Art. no. eaar5438.

[39] T. Elery, S. Rezazadeh, C. Nesler, and R. D. Gregg, "Design and validation of a powered Knee–Ankle prosthesis with high-torque, low-impedance actuators," *IEEE Trans. Robot.*, vol. 36, no. 6, pp. 1649–1668, Dec. 2020.